Bulg. J. Phys. **42** (2015) 305–314

Photoionization of Diamond Interacting with Intense 30fs Laser Pulse

B. Obreshkov, T. Apostolova
Institute of Nuclear Research and Nuclear Energy, Bulgarian Academy of Sciences, 72 Tsarigradsko Chaussee, BG-1784 Sofia, Bulgaria

Received *7 August 2015*

Abstract. We investigate numerically the photionization of diamond irradiated by 800 nm intense 30fs laser pulse. We find that ionization depends sensitively on the characteristics of the substrate band structure and that the electron yield changes non-monotonically with the increase of the laser intensity. For low intensity of the light pulse $I \sim 10^{12}$ W/cm^2, we find that carrier generation occurs via absorption of 9 photons. When the intensity of the laser pulse is higher than 5×10^{13} W/cm^2, the creation of electron-hole pairs is highly efficient resulting in carrier densities exceeding the critical density $n \sim 10^{20}$ cm^{-3} for dielectric breakdown of bulk diamond.

PACS codes: 77.22.Jp, 79.20.-m, 81.05.ug

1 Introduction

The availability of intense ultrashort laser pulses has allowed the observation of chemical reactions and non-thermal phase transitions occurring on femto- and pico-second time scales [1]. In the excitation with ultrashort laser pulses, energy is transferred to the electrons and next to the lattice of the substrate ionic cores. For a relatively short duration of the laser pulse $\tau_L \sim 10$ fs, the nuclei remain fixed at the lattice points and the substrate absorbs energy from the field due to the creation of electron-hole pairs. For the specific laser wavelength, the electron-hole plasma density can become high enough resulting in efficient energy transfer from the laser to the electrons eventually causing dielectric breakdown [2–4].

The conventional theoretical description of strong-field ionization is based on the Keldysh approach [5], which unifies multiphoton with tunneling ionization. At the same time this approach provides a framework for quantitative analysis of ionization for a wide range of light-matter interactions, including optical breakdown [6], high-order harmonic generation [7], laser ablation and nanostructuring [8]. It also relies on appropriate approximation for the dispersion relation between energy and momentum of Bloch electrons, and more recently

it has been shown that photionization may depend sensitively on details of the substrate band structure [9, 10].

The purpose of this paper is to numerically investigate the photoionization of diamond subjected to intense 30fs laser field by incorporating realistic substrate band structure. We neglect dissipative processes due to electron-phonon couplings, impurity and disorder scattering on longer time scales (> 10 fs), and also neglect relaxation and dissipation in the interacting many-electron system. In long-wavelength approximation we represent the light pulse by a spatially uniform time-dependent electric field and describe the electronic motion quantum-mechanically by the time-dependent Schrödinger equation in single-particle approximation. The paper is organized as follows: in Sec. II, we outline our theoretical approach, in Sec. III we discuss numerical results for the photoionization yield and Sec. IV includes our main conclusions.

2 Theoretical Model

We model the interaction of the macroscopic pulsed laser field with bulk diamond in one-electron approximation based on the Hamiltonian

$$H(t) = \frac{1}{2}(\mathbf{p} + \mathbf{A}(t))^2 + V(\mathbf{r}) \tag{1}$$

including the lattice-periodic ionic potential

$$V(\mathbf{r}) = \sum_{\mathbf{G}} V(G) \cos(\mathbf{G} \cdot \boldsymbol{\tau}) e^{i\mathbf{G}\cdot\mathbf{r}}, \tag{2}$$

where $\boldsymbol{\tau} = a_0(1/4, 1/4, 1/4)$ is a relative vector connecting two carbon atoms in a crystal unit cell, $a_0 = 3.57$ Å is the bulk lattice constant for diamond and $\mathbf{G}$ labels the reciprocal lattice wave-vectors. We apply the empirical pseudopotential method to describe the atomic formfactors $V(G)$ [11,12]. Velocity gauge is used throughout our calculation [13] and the time-dependent wave-function is expanded over Bloch states with definite crystal momentum $\mathbf{k}$

$$\psi(\mathbf{r}, t) = \sum_{n\mathbf{k}} a_{n\mathbf{k}}(t) e^{i\mathbf{k}\cdot\mathbf{r}} u_{n\mathbf{k}}(\mathbf{r}), \tag{3}$$

where $u_{n\mathbf{k}}$ is lattice-periodic part of the Bloch wave-function

$$u_{n\mathbf{k}}(\mathbf{r}) = \sum_{\mathbf{G}} e^{i\mathbf{G}\cdot\mathbf{r}} c_{n,\mathbf{G}+\mathbf{k}}, \tag{4}$$

given in terms of Fourier coefficients satisfying

$$\frac{1}{2}(\mathbf{G} + \mathbf{k})^2 c_{n,\mathbf{G}+\mathbf{k}} + \sum_{\mathbf{G}'} V_{\mathbf{G}-\mathbf{G}'} c_{n,\mathbf{G}'+\mathbf{k}} = \varepsilon_{n\mathbf{k}} c_{n,\mathbf{G}+\mathbf{k}}, \tag{5}$$

with eigen-energies $\varepsilon_{n\mathbf{k}}$ specifying the static substrate band structure. The time-evolution of the Fourier amplitudes

$$i\partial_t a_{n\mathbf{k}}^{(m\mathbf{k})}(t) = \varepsilon_{n\mathbf{k}} a_{n\mathbf{k}}^{(m\mathbf{k})}(t) + \sum_{n'} \mathbf{A}(t)\cdot \mathbf{p}_{nn'}(\mathbf{k}) a_{n'\mathbf{k}}^{(m\mathbf{k})}(t), \tag{6}$$

is subject to initial conditions specified long before the start of the pulse $a_{n\mathbf{k}}^{(m\mathbf{k})}(t\to-\infty) = \delta_{nm}$ and the matrix representation of the momentum operator is

$$\mathbf{p}_{nn'}(\mathbf{k}) = \mathbf{k}\delta_{nn'} - i\frac{1}{\Omega_{u.c.}}\int_{\Omega_{u.c.}} d^3\mathbf{r} u_{n\mathbf{k}}^*(\mathbf{r})\nabla_{\mathbf{r}} u_{n'\mathbf{k}}(\mathbf{r}), \tag{7}$$

with off-diagonal matrix elements describing interband transitions, $\Omega_{u.c.} = a_0^3/4$ is the volume of the unit cell. The occupation numbers of single-particle states at time t are

$$f_{n\mathbf{k}}(t) = \sum_{m=1}^{M} |a_{n\mathbf{k}}^{(m\mathbf{k})}(t)|^2, \tag{8}$$

where M is the total number of in initially occupied valence bands. The total number of electrons that have been photo-excited into the conduction band is given by the Brillouin zone integral

$$n_e(t) = \sum_{n=M+1}^{\infty} \int_{\mathrm{BZ}} \frac{d^3\mathbf{k}}{(2\pi)^3} f_{n\mathbf{k}}(t). \tag{9}$$

Charge neutrality implies that the total number of valence band holes is equal to the total number of conduction electrons, i.e. $n_h = n_e$.

3 Numerical Result and Discussion

We evaluate the substrate band structure in a plane-wave basis with kinetic-energy cut-off 35 Ry. The pseudopotential formfactors $V(G)$ used for diamond (in Rydbergs) are $V(G^2=3) = -0.625$, $V(G^2=8) = 0.051$ and $V(G^2=11) = 0.206$, here the wave-number G is given in units of $2\pi/a_0$. The time-dependent electron density is represented in a basis of static Bloch orbitals including 4 valence and 16 conduction bands, the time-integration of the Schrödinger equation is performed by applying the Cranck-Nicholson method for small equidistant time steps $\delta t \approx 1$ attosecond. The Brillouin zone integration is performed by a simple Monte Carlo method including 1500 randomly generated $\mathbf{k}$-points in a cube of edge length $(4\pi/a_0)$. The time-profile of the laser field is modelled by a Gaussian function

$$\mathbf{A}(t) = \mathbf{e}A_0 \sin(\omega_L t) e^{-\ln(4)(t-t_0)^2/\tau_L^2}, \tag{10}$$

where $\mathbf{e}$ is unit vector pointing in the direction of the electric field, the driving frequency is $\hbar\omega_L = 1.55$ eV, $\tau_L = 30$ fs, t_0 specifies the instant of peak intensity

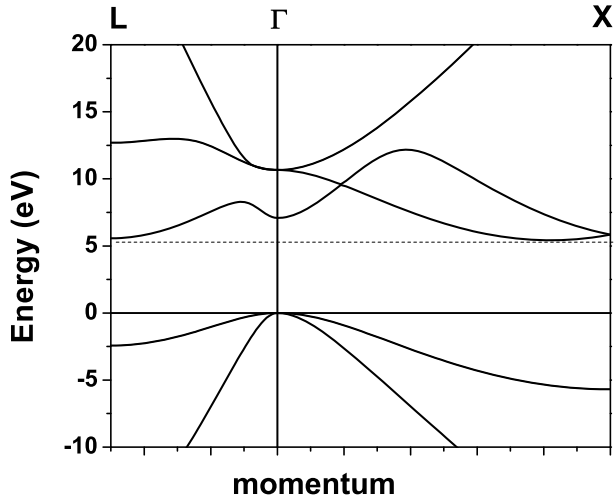

Figure 1. Static band structure of diamond along the ΓX and ΓL directions in the Brillouin zone. The crystal momentum is given in of units of $2\pi/a_0$.

I of the laser field, the field strength A_0 is related to $I = c\omega_L^2 A_0^2/(8\pi)$ and c is the speed of light in vacuum.

In Figure 1, we show the band structure for crystal momentum $\mathbf{k}$ changing along the ΓX and ΓL directions in the Brillouin zone. The empirical pseudopotential model reproduces quantitatively the principal energy gaps of this band structure. The location of the conduction band minimum at $\mathbf{k} = (0.8, 0, 0)2\pi/a_0$ corresponding to an indirect gap of 5.42 eV is in very good quantitative agreement with the experimental result ($E_{\rm gap} = 5.45$ eV). Since in long-wavelength approximation the laser cannot induce a momentum changing transition, the minimal energy required to surpass the energy gap at the Γ point is 7 eV. For relatively low intensity of the laser field $I \ll 10^{14}$ W/cm^2, excitation of valence electrons across this gap should occur via 5 photon absorption according to the Keldysh theory [5].

In Figure 2 we show the time evolution of the electron density $n_e(t)$ for three different intensities of the applied laser field. The total number of electrons entering the conduction band increases on the rising part of the pulse. At a later time, the charge density oscillations follow the time periodicity of the incident radiation. As we show below these transient charge oscillations are due to the time-dependent shift of the momenta of valence electrons $\mathbf{k} \to \mathbf{k} + \mathbf{A}(t)$, which adjust instantaneously (adiabatically) to the slow variation of the vector potential. Due to this velocity boost, the overlap among shifted valence and undistorted conduction bands $\langle c\mathbf{k}|v\mathbf{k}(t)\rangle$ oscillates with the periodicity of the laser field. Noticeably, during one half-cycle of the pulse, some fraction of electrons

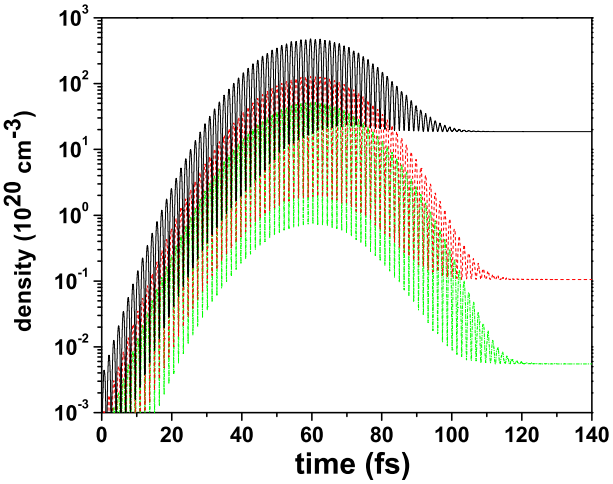

Figure 2. Time-evolution of the electron density for three different peak intensities of 30fs laser pulse interacting with diamond. $I = 5\times10^{12}$ W/cm^2 (green line), $I = 10^{13}$ W/cm^2 (red line) and $I = 5 \times 10^{13}$ W/cm^2 (black line).

are transferred back into the valence band and deviation from purely adiabatic time-evolution occurs at the extrema of the electric field. The photo-ionization yield stabilizes in the wake of the pulse. Photoionization is less likely for lower field intensities ($I < 10^{13}$ W/cm^2), since valence electrons do not gain sufficient energy from the field to be excited into the conduction band. That is because of the wide bandgaps of diamond, which favor adiabatic time evolution resulting in relatively small final electron yields $n_e \sim 10^{18}$ cm^{-3}. Non-adiabatic effects of electron-hole pair creation depend very sensitively on the laser intensity, for instance when $I > 5 \times 10^{13}$ W/cm^2 the occupation of the conduction band becomes prominent resulting in high photoionization yields with $n_e \sim 10^{21}$ cm^{-3} after the conclusion of the pulse.

To analyze such non-adiabatic effects in the electron dynamics, we diagonalize the time-dependent Hamiltonian $H(t)|n\mathbf{k}(t)\rangle = \varepsilon_n(\mathbf{k}(t))|n\mathbf{k}(t)\rangle$ in terms of accelerated Bloch states with $\mathbf{k}(t) = \mathbf{k} + \mathbf{A}(t)$, here $\mathbf{k}$ is the initial crystal momentum of valence electrons long before the start of the pulse. In a simplified two band model with one valence and one conduction band, the adiabatic time evolution does not produce any real excitation of the crystal, thus the probability for virtual creation of an electron-hole pair at time t is

$$P_{\mathrm{ad}}(t) = \int_{BZ} \frac{d^3\mathbf{k}}{(2\pi)^3} |\langle c\mathbf{k}|v\mathbf{k}(t)\rangle|^2. \tag{11}$$

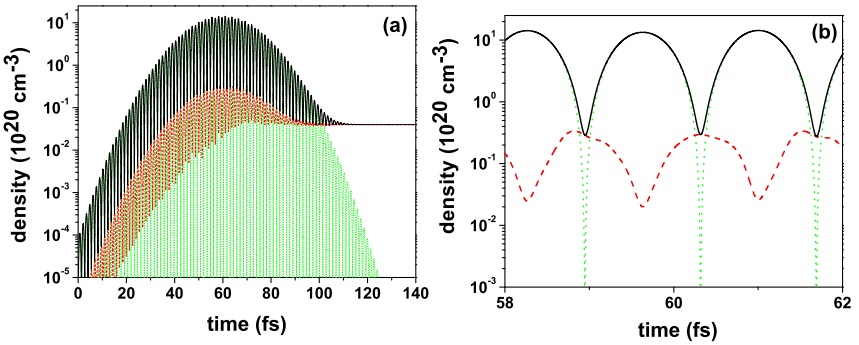

Figure 3. Contributions to the total electron density for laser pulse intensity $I = 10^{13}$ W/cm^2: (a) Non-adiabatic (red line) versus adiabatic fraction (green curve), the black line gives the total electron yield; (b) shows the time evolution of the fractions near the peak intensity of laser field.

The probability for non-adiabatic transition is given by a Brillouin zone integral

$$P_{\rm non-ad}(t) = \int_{BZ} \frac{d^3\mathbf{k}}{(2\pi)^3} \times \left| \int_{-\infty}^{t} dt' \exp\Big(-i \int_{-\infty}^{t'} dt'' [\varepsilon_v(\mathbf{k}(t'')) - \varepsilon_c(\mathbf{k}(t''))] \Big) M_{cv}(\mathbf{k}(t')) \right|^2, \quad (12)$$

with non-adiabatic coupling induced by the electric field $\mathbf{E}(t) = -\partial_t \mathbf{A}(t)$,

$$M_{cv}(\mathbf{k}(t)) = \frac{\mathbf{E}(t) \cdot \mathbf{p}_{cv}(\mathbf{k}(t))}{\varepsilon_c(\mathbf{k}(t)) - \varepsilon_v(\mathbf{k}(t))}. \quad (13)$$

In Figure 3 we plot the adiabatic and non-adiabatic contributions to the transient electron density for electric field polarized parallel to C-C bonds with intensity $I = 10^{13}$ W/cm^2. The time oscillations of the electron density exhibited in the adiabatic fraction are exclusively due to the acceleration of valence electrons in the radiation field. The non-adiabatic fraction due to real electron-hole pair excitations does not generally follow the temporal profile of the pulse. It is much smaller in magnitude than the adiabatic one (justifying the use of Keldysh theory for photoionization), and is most effective at the extrema of the electric field causing promotion of valence electrons into the conduction band (with carrier densities $n \sim 10^{19}$ cm^{-3}).

The momentum distribution of photoionized electrons at the end of the pulse is shown in Figure 4 for two specific directions in the bulk Brillouin zone and for two different polarizations of the laser field: either parallel or perpendicular to C-C bonds. For the lower intensity $I = 10^{13}$ W/cm^2, Figures 4(a-b) give the

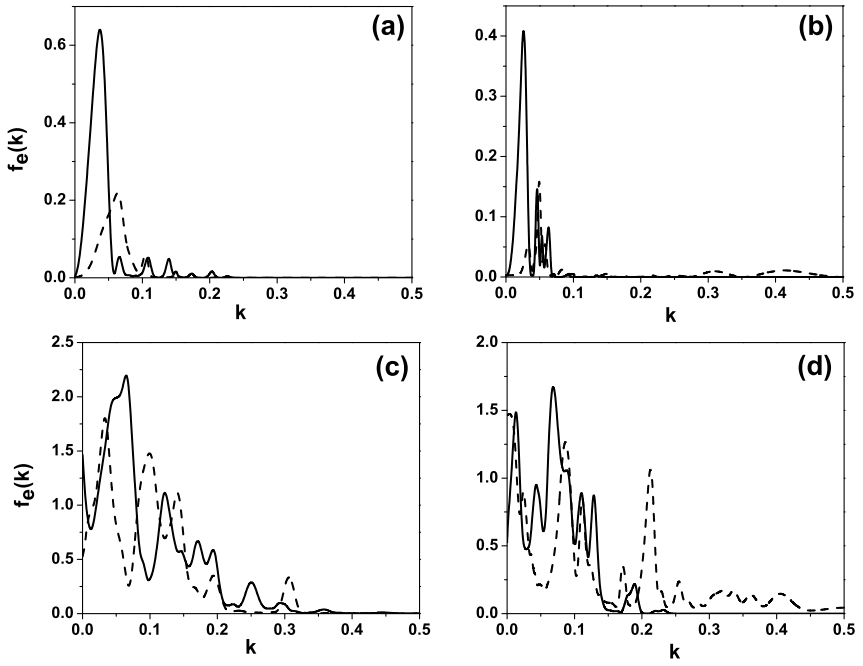

Figure 4. (a) Momentum distribution of photoionized electrons emerging along the ΓX direction after the irradiation of diamond with 30fs laser pulse linearly polarized either parallel (solid line) or perpendicular to bonds between carbon atoms (dashed line). The pulse intensity is $I = 10^{13}$ W/cm^2; (c) gives the same distributions for $I = 5 \times 10^{13}$ W/cm^2; (b) and (d) give momentum distribution of conduction electrons emerging in the ΓL direction for pulse intensity $I = 10^{13}$ W/cm^2 and $I = 5 \times 10^{13}$ W/cm^2, respectively. The crystal momentum $\mathbf{k}$ is given in units of $2\pi/a_0$.

distribution of electrons emerging with momenta $\mathbf{k}$ in the ΓX ΓL directions, respectively. For low intensity, photoionization favors states close to the Brillouin zone centre, the occupation of the conduction bands depends weakly on the polarization of the radiation field. If the intensity is increased to 5×10^{13} W/cm^2, cf. Figures 4(c-d), the distributions broaden in momentum space and move towards the edges of the Brillouin zone. The sharp structures exhibited at higher momenta in the carrier distribution prove that significant contribution to the total electron yield is due to transitions not occurring in the centre of the Brillouin zone. This is also consistent with semi-analytic results for photoionization of dielectrics irradiated with short laser pulses at moderate field intensities [14].

The density of conduction band states after the conclusion of the pulse is shown in Figure 5. Figure 5(a) gives the density of states for the lower field intensity $I = 10^{13}$ W/cm^2 including both parallel and perpendicular polarization of the laser. If the electric field is polarized parallel to C-C bonds, the distribution

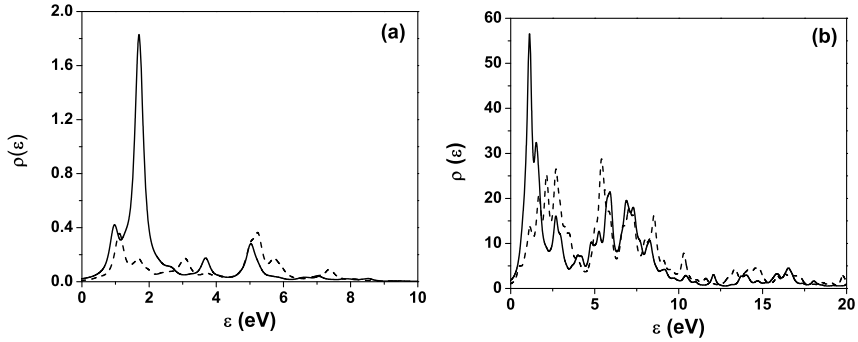

Figure 5. Density of conduction band states after the irradiation of diamond with 30fs laser pulse: (a) the peak intensity of the laser pulse is $I = 10^{13}$ W/cm^2; and (b) it is $I = 5 \times 10^{13}$ W/cm^2. The kinetic energy ε of the released electrons is measured relative to the conduction band minimum.

shows characteristic low energy peak located at 1.5 eV above the conduction band minimum, reflecting the fact that in this regime transitions occur near the Brillouin zone centre. Though the electron distribution becomes more diffuse for perpendicularly polarized electric field, this polarization dependence tends to average out in the final photoionization yield. For the higher pulse intensity $I = 5 \times 10^{13}$ W/cm^2 shown in Figure 5(b), the distribution exhibits a pronounced energy tail of electrons with kinetic energies extending up to 15 eV above the conduction band minimum. The excess kinetic energy of the photoexcited carriers favors the impact ionization in which additional electron-hole pairs are created after the end of the pulse.

In Figure 6 we show the photionization yield as a function of the pulse intensity I for parallel polarization of the electric field. In the low intensity regime $I < 1$ TW/cm^2, the electron yield increases linearly with the increase of I due to highly suppressed one-photon ionization process (with negligible final densities $n \leq 10^{14}$ cm^{-3}). The photoionization probability raises steeply with the increase of the intensity in the range $I \in [1, 2]$ TW/cm^2. The slope of the theoretical curve can be fitted to $n \sim I^N$ scaling law over that range, with $N = 9$ corresponding to 9-photon ionization. For such relatively weak field strength, photo-ionization favors states close to the Brillouin zone centre, such that to surpass the 7 eV energy gap at the Γ point requires $N = 5$ photon absorption (for the 800 nm laser wavelength). However we find ionization requires 4 photons in excess, pointing out that electron promotion across the diamond bandgaps is sensitive to the shape of the band-structure away from the Brillouin zone centre during the transition (cf. also [9, 15]). At $I \approx 3$ TW/cm^2 ionization becomes unlikely, since the electron yield decreases by nearly one-order of magnitude. That is primary because interband transitions occur away from the Γ point, where the wide bandgaps of diamond (~ 10 eV) suppress ionization.

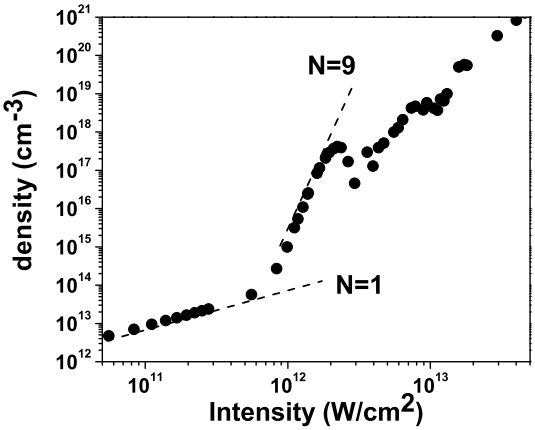

Figure 6. Intensity dependence of the photoionization yield after the irradiation of diamond with 30fs laser pulse linearly polarized parallel to bonds between carbon atoms.

For increased peak intensities of the light pulse $I > 5$ TW/cm^2, the slope of the curve flattens out as function of I. In this high-intensity regime, the energy and momentum distribution of ionized electrons become more diffuse and extend over the entire Brillouin zone. When $I = 5 \times 10^{13}$ W/cm^2 the carrier densities are $n \geq 10^{20}$ cm^{-3}, pointing out that optical breakdown occurs [4]. For high conduction electron density, the corresponding plasma frequency in bulk matches the laser frequency ω_L, so that the electrons can absorb energy from the laser pulse very efficiently.

4 Conclusion

We investigated photoionization of bulk diamond irradiated with 800 nm intense 30fs laser pulse. For intensities $I < 10^{13}$ W/cm^2, we find that electron dynamics follows the adiabatic time evolution, when the conduction electron density displays a pronounced oscillatory behavior due to transient polarization of the solid. We find that non-adiabatic effects of electron-hole pair excitation depend very sensitively on the characteristics of the substrate band structure. In particular we find that electrons are excited across the diamond bandgaps by absorbing 9 photons. For this specific wavelength, we also find suppression of ionization at specific intensity threshold $I = 3$ TW/cm^2. For higher intensities $I > 10^{13}$ W/cm^2, we show that non-adiabatic effects become prominent causing optical breakdown of diamond creating many electron-hole pairs.

Acknowledgement

This material is based upon work supported by the Air Force Office of Scientific Research, Air Force Material Command, USAF under Award No. FA9550-15-1-0197 (T.A.). The authors want to thank the organizers for providing a slot to give a talk on "Photoionization of diamond interacting with intense ultrashort laser field" in commemoration of the 75th anniversary of Prof. Matey Mateev. T.A. also acknowledges DFNI-E02/6.

References

[1] S.K. Sundaram and E. Mazur (2002) *Nature Mater*. **1** 217.
[2] T. Apostolova and Y. Hahn (2000) *J. Appl. Phys*. **88** 1024.
[3] A. Kaiser, B. Rethfeld, M. Vicanek, and G. Simon (2000) *Phys. Rev. B* **61** 11437.
[4] T. Otobe, M. Yamagiwa, J.-I. Iwata, K. Yabana, T. Nakatsukasa, G. F. Bertsch (2008) *Phys. Rev. B* **77** 165104.
[5] L. V. Keldysh (1965) *Sov. Phys. – JETP* **20** 1307.
[6] M. Lenzner, J. Krüger, S. Sartania, Z. Cheng, C. Spielmann, G. Mourou, W. Kautek, and F. Krausz (1998) *Phys. Rev. Lett*. **80** 4076.
[7] T. Brabec and F. Krausz (2000) *Rev. Mod. Phys*. **72** 545.
[8] J. Reif (2010) *Laser-Surface Interactions for New Materials Production*, Springer Series in Materials Science **130**, p. 19, Springer-Verlag Berlin Heidelberg.
[9] V.E. Gruzdev (2007) *Phys. Rev. B* **75** 205106.
[10] P.A. Zhokhov and A.M. Zheltikov (2014) *Phys. Rev. Lett*. **113** 133903.
[11] W. Slaslow, T.K. Bergstresser and M. Cohen (1966) *Phys. Rev. Lett*. **16** 354.
[12] G. Pennigton and N. Goldsman (2001) *Phys. Rev. B* **64** 045104.
[13] J.B. Krieger and G.J. Iafrate (1986) *Phys. Rev. B* **33** 5494.
[14] C. Mézel, G. Duchateau, G. Geneste, and B. Siberchicot (2013) *J. Phys: Condensed Matter* **25** 235501.
[15] P.G. Hawkins and M.Yu. Ivanov (2013) *Phys. Rev. A* **87** 063842.